Nuclear magnetic resonance magnetic dipolar spectral density functions for two-dimensional lattice diffusion: hexagonal systems

1998 J. Phys.: Condens. Matter 10 417

(http://iopscience.iop.org/0953-8984/10/2/021)

J. Phys.: Condens. Matter **10** (1998) 417–428. Printed in the UK PII: S0953-8984(98)87020-3

Nuclear magnetic resonance magnetic dipolar spectral density functions for two-dimensional lattice diffusion: hexagonal systems

D H MacDonald†, C A Sholl† and P C L Stephenson‡

† Division of Physics and Electronics Engineering, University of New England, Armidale, NSW 2351, Australia

‡ School of Physical Sciences, University of Kent, Canterbury, Kent CT2 7NR, UK

Received 19 August 1997

Abstract. Previous calculations of spectral density functions for like-spin magnetic dipolar interactions between spins undergoing two-dimensional diffusion are extended to the hexagonal lattice and the honeycomb structure. The diffusion models used are the random-walk and mean-field models. Analytic approximations to the functions are obtained. It is shown that the simple function proposed by Richards cannot provide good accuracy over the whole range of frequency and temperature, and a modified function is suggested.

1. Introduction

Nuclear spin relaxation is an excellent technique for detecting and analysing two-dimensional diffusion. In the low-frequency or high-temperature limits the spectral density functions of the microscopic field fluctuations, and the consequent relaxation rates, have a logarithmic frequency dependence which is characteristic of two-dimensional diffusion (Sholl 1981). This has been used to show, using a variety of spin-relaxation techniques, that diffusion is essentially two dimensional in some intercalation compounds and layered compounds and on some crystal surfaces (see, for example, Heitjans *et al* (1991), McDowell *et al* (1995), Ebinger *et al* (1996), Kimmerle *et al* (1997) and references therein). The logarithmic frequency dependence is sufficient to confirm that the diffusion is two dimensional, but the form of the spectral density function over the entire range of frequencies is required to deduce details of the diffusion, such as the mean atom jump rate and the contribution to the diffusion from jumps between planes.

A simple spectral density function of the form $\log[1 + 1/(\omega\tau)^2]$, where τ is the mean jump rate, has been suggested by Richards (1978) for two-dimensional diffusion. This function has the correct functional form for both large and small $\omega\tau$, but it will not necessarily show the correct rate of approach to the limits and its accuracy for intermediate ranges of $\omega\tau$ is not clear. Detailed calculations of spectral density functions are required to provide a firm basis for analysing relaxation data over the entire range of temperature and frequency, and to assess the accuracy of simple approximations such as that due to Richards. Spectral density functions for like-spin magnetic dipolar interactions between spins undergoing two-dimensional diffusion on a square lattice, have been obtained by Stephenson and Sholl (1993) (to be referred to as SS). These calculations were carried out for random-walk and mean-field diffusion models and were compared with previous

0953-8984/98/020417+12$19.50

continuum diffusion theories. The mean-field results provide exact spectral density functions in the limit of low concentration of diffusing spins and provide a reasonable approximation at other spin concentrations.

Two-dimensional diffusion commonly occurs in hexagonal systems and the aim of this paper is to extend the previous calculations to models of diffusion on the hexagonal lattice and the honeycomb structure. The extension to the hexagonal lattice is a straightforward application of the theory, but the honeycomb structure introduces complications because it is not a Bravais lattice.

The next section describes the dependence of the spectral density functions on the magnetic field direction, and outlines the general method of calculation of the functions for a crystal with several sites per unit cell. The following section evaluates expressions for the probability functions required for each of the random-walk and mean-field models. The results are then presented and analytic approximations are given which allow the spectral density functions to be easily reproduced. It is shown that the simple function suggested by Richards cannot provide good accuracy over the entire range, and a modification of it is suggested.

2. Spectral density functions

The spectral density functions $J^{(p)}(\omega)$ depend on the orientation of the applied magnetic field with respect to the plane of diffusion. For the hexagonal lattice and the honeycomb structure the functional dependence is (SS, Sholl 1986)

$$d_0^{-2}J^{(0)}(\omega) = J_{00}(\omega) - 3J_{00}(\omega)\sin^2\theta + \frac{3}{4}[3J_{00}(\omega) + J_{22}(\omega)]\sin^4\theta \tag{1}$$

$$d_1^{-2}J^{(1)}(\omega) = \frac{1}{2}[3J_{00}(\omega) + 2J_{22}(\omega)]\sin^2\theta - \frac{1}{2}[3J_{00} + J_{22}(\omega)]\sin^4\theta \tag{2}$$

$$d_2^{-2}J^{(2)}(\omega) = J_{22}(\omega) - J_{22}(\omega)\sin^2\theta + \frac{1}{8}[3J_{00}(\omega) + J_{22}(\omega)]\sin^4\theta \tag{3}$$

where θ is the angle between the applied field and the normal to the plane, and $d_0^2 = 16\pi/5$, $d_1^2 = 8\pi/15$, $d_2^2 = 32\pi/15$. The functions $J_{00}(\omega)$ and $J_{22}(\omega)$ are defined by

$$J_{pp}(\omega) = c\sum_{\alpha,\beta}\frac{Y_{2p}^*(\Omega_\alpha)}{r_\alpha^3}\frac{Y_{2p}(\Omega_\beta)}{r_\beta^3}P(\boldsymbol{r}_\alpha, \boldsymbol{r}_\beta, \omega) \tag{4}$$

where c is the fraction of sites occupied by spins, $Y_{2p}(\Omega)$ are normalized spherical harmonics relative to the normal to the plane and $P(\boldsymbol{r}_\alpha, \boldsymbol{r}_\beta, \omega)$ is the real part of the complex Fourier transform

$$P_c(\boldsymbol{r}_\alpha, \boldsymbol{r}_\beta, \omega) = 2\int_0^\infty P(\boldsymbol{r}_\alpha, \boldsymbol{r}_\beta, t)\mathrm{e}^{\mathrm{i}\omega t}\,\mathrm{d}t \tag{5}$$

of $P(\boldsymbol{r}_\alpha, \boldsymbol{r}_\beta, t)$, which is the probability of a pair of spins being separated by $\boldsymbol{r}_\beta$ a time t after they were separated by $\boldsymbol{r}_\alpha$. The relaxation rates are linear combinations of these spectral density functions (see, for example, Sholl 1986).

The angular dependence of $J^{(p)}(\omega)$ in equations (1)–(3) is appropriate for nuclear spin-relaxation experiments using single crystals. For polycrystalline samples, it is a reasonable approximation to replace the average over relaxation rates by an average over the spectral density functions (Barton and Sholl 1976), and each of the $J^{(p)}(\omega)$ then become $d_p^2(J_{00}(\omega) + 2J_{22}(\omega))/5$.

As described in SS, an efficient practical approach for the evaluation of equation (4) is to use a reciprocal-space formalism. The extension of this theory to non-Bravais lattices

requires consideration of the possible types of relative separation of a pair of diffusing spins in relation to the basis of the crystal structure. For a basis of B sites per unit cell there are B^2 types of separation of a pair of spins for each of $\boldsymbol{r}_\alpha$ at time zero and $\boldsymbol{r}_\beta$ at time t. The reciprocal-space expression for $J_{pp}(\omega)$ for non-Bravais lattices then becomes

$$J_{pp}(\omega) = \frac{1}{(2\pi)^4}\frac{c}{B^2}\sum_{m,n=1}^{B^2}\int\int \mathrm{d}\boldsymbol{q}\ \mathrm{d}\boldsymbol{q}'\ T_p^*(\boldsymbol{q}, \boldsymbol{j}_m)T_p(\boldsymbol{q}', \boldsymbol{j}_n)P_{mn}(\boldsymbol{q}, \boldsymbol{q}', \omega) \tag{6}$$

where $P_{mn}(\boldsymbol{q}, \boldsymbol{q}', \omega)$ is the temporal and spatial Fourier transform of $P(\boldsymbol{r}_\alpha, \boldsymbol{r}_\beta, t)$ for a pair of spins with a separation of type m at time zero and a separation of type n at time t. It has been assumed that the probability of occupation of a site by a spin is the same for all sublattices. The functions $T_p(\boldsymbol{q}, \boldsymbol{j})$ are the Fourier transforms of $Y_{2p}(\Omega_\alpha)/r_\alpha^3$ for spins separated by $\boldsymbol{l}+\boldsymbol{j}$, where $\boldsymbol{l}$ is a lattice vector, and expressions for their evaluation are given in the appendix of SS. The integrals are over the first Brillouin zone of the reciprocal lattice, with the area element $\mathrm{d}\boldsymbol{q} = A\ \mathrm{d}q_1\ \mathrm{d}q_2$, where A is the area of the two-dimensional unit cell.

Care must be taken in the use of $P(\boldsymbol{q}, \boldsymbol{q}', \omega)$ in equation (6). The real part of the temporal Fourier transform is required, but this cannot be obtained by taking the real part of $P_c(\boldsymbol{q}, \boldsymbol{q}', \omega)$ when $P(\boldsymbol{q}, \boldsymbol{q}', t)$ is complex, which can occur for non-Bravais lattices. The appropriate procedure is to evaluate $[P_c(\boldsymbol{q}, \boldsymbol{q}', \omega) + P_c(\boldsymbol{q}, \boldsymbol{q}', -\omega)]/2$ and use this form in equation (6).

The simplest lattice diffusion model is the random-walk model for which each of a pair of spins is assumed to undergo a random walk with a mean time τ_s between jumps. Both spins may therefore occupy a particular site in this model, but this case is excluded from contributing to the expression (6) through the definition of $T_p(\boldsymbol{q}, \boldsymbol{j})$. The site-blocking effects of a pair of spins are correctly taken into account in the mean-field model, which provides an exact analysis of the lattice diffusion of a pair of spins on a lattice. The mean-field model therefore provides an exact calculation of the spectral density functions in the limit of low spin concentrations. An approximation for an arbitrary spin concentration c is obtained by using the mean-field results with τ_s taken as the mean time between jumps of a spin at that spin concentration; the correlations between the diffusion of a pair of spins and all other spins are then included in an average manner. Random-walk and mean-field expressions for the diffusion probabilities are obtained in the next section for diffusion on the hexagonal lattice and honeycomb structure.

3. Probability functions

3.1. The hexagonal lattice

The probability functions $P(\boldsymbol{q}, \boldsymbol{q}', \omega)$ for the hexagonal lattice are a straightforward application of the theory described in SS for the square lattice, for both the random-walk and mean-field models. The random-walk expression for $P(\boldsymbol{q}, \boldsymbol{q}', \omega)$ for any Bravais lattice is

$$P_{RW}(\boldsymbol{q}, \boldsymbol{q}', \omega) = \frac{2(2\pi)^2\tau\,[1-\phi(\boldsymbol{q})]}{[1-\phi(\boldsymbol{q})]^2 + (\omega\tau)^2}\delta(\boldsymbol{q}-\boldsymbol{q}') \tag{7}$$

where $\tau = \tau_s/2$, with τ_s the mean time between jumps of a single spin, $\phi(\boldsymbol{q})$ is the lattice structure factor given by

$$\phi(\boldsymbol{q}) = \sum_k w_k \exp(-\mathrm{i}\boldsymbol{q}\cdot\boldsymbol{r}_k) \tag{8}$$

and w_k is the probability that a jump of a spin at the origin will be to $\boldsymbol{r}_k$. For the hexagonal lattice, with a 120° unit cell and lattice parameter a, the values of w_k are 1/6 and

$$\phi(\boldsymbol{q}) = \frac{1}{3}\left[\cos q_1 a + \cos q_2 a + \cos(q_1 + q_2)a\right]. \tag{9}$$

The mean-field theory gives an integral equation with a separable kernel for $P(\boldsymbol{q}, \boldsymbol{q}', \omega)$ and the method of solution is similar to that used by SS, Barton and Sholl (1976) and Fedders and Sankey (1978). The solution is

$$P_{\mathrm{mf}}(\boldsymbol{q}, \boldsymbol{q}', \omega) = P_{\mathrm{rw}}(\boldsymbol{q}, \boldsymbol{q}', \omega) + \frac{2}{3\tau}\Re\left\{d_0(\boldsymbol{q}, \omega)d_0(\boldsymbol{q}', \omega)\sum_{i,j=1}^{3} L_{ij}(\omega) f_i(\boldsymbol{q}) f_j(\boldsymbol{q}')\right\} \tag{10}$$

where the functions $d_0(\boldsymbol{q}, \omega)$ and $f_i(\boldsymbol{q})$ are

$$d_0(\boldsymbol{q}, \omega) = \frac{\tau}{[1 - \phi(\boldsymbol{q}]) - \mathrm{i}\omega\tau} \tag{11}$$

$$f_1(\boldsymbol{q}) = 1 - \cos q_1 a \tag{12}$$

$$f_2(\boldsymbol{q}) = 1 - \cos q_2 a \tag{13}$$

$$f_3(\boldsymbol{q}) = 1 - \cos(q_1 + q_2)a. \tag{14}$$

Expressions for $L_{ij}(\omega)$ are given in the appendix.

3.2. The honeycomb structure

The honeycomb structure may be described as two displaced hexagonal lattices as shown in figure 1. The vectors $\boldsymbol{a}_1$ and $\boldsymbol{a}_2$ are the basis of one hexagonal lattice, with $a_1 = a_2 = \sqrt{3}a$, where a is the length of a segment of a honeycomb hexagon. The sites on this lattice will be denoted as type 1 sites. The second hexagonal lattice is displaced from this lattice by $\boldsymbol{b} = (\boldsymbol{a}_1 + 2\boldsymbol{a}_2)/3$ and these lattice sites will be denoted as type 2 sites. The complete set of type 1 and type 2 sites form the honeycomb structure. Each site has three nearest neighbours: for type 1 sites they are $\boldsymbol{b} - \boldsymbol{p}_k$ and for type 2 sites they are $\boldsymbol{b} + \boldsymbol{p}_k$, where $\boldsymbol{p}_1 = 0, \boldsymbol{p}_2 = \boldsymbol{a}_2$ and $\boldsymbol{p}_3 = \boldsymbol{a}_1 + \boldsymbol{a}_2$, which are hexagonal-lattice vectors.

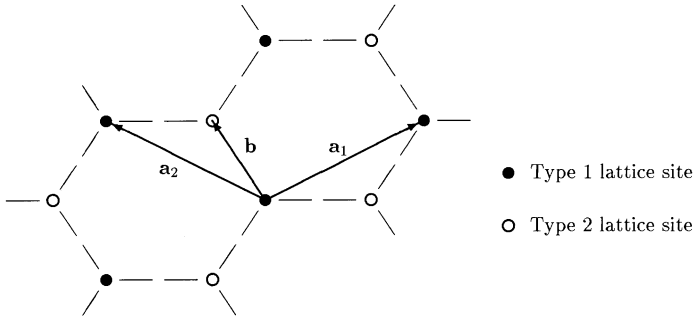

Figure 1. The honeycomb structure as a superposition of two hexagonal lattices separated by $\boldsymbol{b} = (\boldsymbol{a}_1 + 2\boldsymbol{a}_2)/3$.

The different types of probability $P(\boldsymbol{r}_\alpha, \boldsymbol{r}_\beta, t)$ will be denoted as $P_{mn}(\boldsymbol{l}, \boldsymbol{l}', t)$ ($m, n = 1$ to 4): $m = 1$ and 2 denotes an initial separation of $\boldsymbol{l}$ with both spins at type 1 and type 2 sites, respectively, $m = 3$ denotes an initial separation of $\boldsymbol{l} + \boldsymbol{b}$ with the spin at the origin a type 1 site and the other spin a type 2 site, $m = 4$ denotes an initial separation of $\boldsymbol{l} - \boldsymbol{b}$

with the spin at the origin a type 2 site and the other spin a type 1 site. A corresponding notation using $\boldsymbol{l}'$ and the index n describes final spin separation types.

The probability functions for the mean-field theory can be obtained from the following rate equations for $P_{mn}(\boldsymbol{l}, \boldsymbol{l}', t)$:

$$\frac{\mathrm{d}P_{mn}(\boldsymbol{l}', t)}{\mathrm{d}t} = -\frac{2}{\tau_s} P_{mn}(\boldsymbol{l}', t) + \frac{[1 - \delta_{l',0}]}{3\tau_s} \sum_{k=1}^{3} \left[P_{m3}(\boldsymbol{l}' - \boldsymbol{p}_k, t) + P_{m4}(\boldsymbol{l}' + \boldsymbol{p}_k, t) \right] \qquad n = 1, 2 \tag{15}$$

$$\frac{\mathrm{d}P_{m3}(\boldsymbol{l}', t)}{\mathrm{d}t} = -\frac{2}{\tau_s} \left[1 - \frac{1}{3} \sum_{k=1}^{3} \delta_{l', -\boldsymbol{p}_k} \right] P_{m3}(\boldsymbol{l}', t) + \frac{1}{3\tau_s} \sum_{k=1}^{3} \left[P_{m1}(\boldsymbol{l}' + \boldsymbol{p}_k, t) + P_{m2}(\boldsymbol{l}' + \boldsymbol{p}_k, t) \right] \tag{16}$$

$$\frac{\mathrm{d}P_{m4}(\boldsymbol{l}', t)}{\mathrm{d}t} = -\frac{2}{\tau_s} \left[1 - \frac{1}{3} \sum_{k=1}^{3} \delta_{l', \boldsymbol{p}_k} \right] P_{m4}(\boldsymbol{l}', t) + \frac{1}{3\tau_s} \sum_{k=1}^{3} \left[P_{m1}(\boldsymbol{l}' - \boldsymbol{p}_k, t) + P_{m2}(\boldsymbol{l}' - \boldsymbol{p}_k, t) \right]. \tag{17}$$

The variable $\boldsymbol{l}$ in $P_{mn}(\boldsymbol{l}, \boldsymbol{l}', t)$ has been suppressed throughout. The Kronecker delta functions in these equations represent the terms for which jumps cannot occur due to site blocking. If these delta functions are omitted, the equations become those for the random-walk theory. The initial conditions for the equations, in the mean-field theory, are

$$P_{mn}(\boldsymbol{l}, \boldsymbol{l}', 0) = 0 \qquad m \neq n \tag{18}$$

$$P_{11}(\boldsymbol{l}, \boldsymbol{l}', 0) = P_{22}(\boldsymbol{l}, \boldsymbol{l}', 0) = \delta_{l,l'}[1 - \delta_{l',0}] \tag{19}$$

$$P_{33}(\boldsymbol{l}, \boldsymbol{l}', 0) = P_{44}(\boldsymbol{l}, \boldsymbol{l}', 0) = \delta_{l,l'}. \tag{20}$$

The initial conditions for the random-walk theory omit the term $\delta_{l',0}$.

Taking the spatial Fourier transform with respect $\boldsymbol{l}$ and $\boldsymbol{l}'$, and the temporal transform (5), of these rate equations and initial conditions gives the matrix equation

$$\mathbf{P}(\boldsymbol{q}, \boldsymbol{q}', \omega)\mathbf{Y}(\boldsymbol{q}', \omega) = \mathbf{X}(\boldsymbol{q}, \boldsymbol{q}', \omega) + \mathbf{D}(\boldsymbol{q}, \boldsymbol{q}') \tag{21}$$

where the elements of $\mathbf{P}$ are the transformed probability functions $P_{mn}(\boldsymbol{q}, \boldsymbol{q}', \omega)$, $\mathbf{D}$ is a diagonal matrix, with elements $D_{11} = D_{22} = D - 4\tau$ and $D_{33} = D_{44} = D$, the matrix $\mathbf{Y}$ and its inverse are

$$\mathbf{Y} = \begin{pmatrix} W & 0 & -\phi^* & -\phi \\ 0 & W & -\phi^* & -\phi \\ -\phi & -\phi & W & 0 \\ -\phi^* & -\phi^* & 0 & W \end{pmatrix}$$

$$\mathbf{Y}^{-1} = N \begin{pmatrix} W^2 - 2\phi\phi^* & 2\phi\phi^* & W\phi^* & W\phi \\ 2\phi\phi^* & W^2 - 2\phi\phi^* & W\phi^* & W\phi \\ W\phi & W\phi & W^2 - 2\phi\phi^* & 2\phi^2 \\ W\phi^* & W\phi^* & 2\phi^{*2} & W^2 - 2\phi\phi^* \end{pmatrix}$$

and D, W and N are

$$D = 4\tau(2\pi)^2\delta(\boldsymbol{q} - \boldsymbol{q}') \tag{22}$$

$$W = 2(1 - \mathrm{i}\omega\tau) \tag{23}$$

$$N = \frac{1}{W[W^2 - 4\phi\phi^*]}. \tag{24}$$

These expressions have been written in terms of $\tau = \tau_s/2$. The elements of the matrix $\mathbf{X}$ are

$$X_{mn}(\boldsymbol{q}, \omega) = -\frac{1}{(2\pi)^2}\int [\phi(\boldsymbol{q}_1)P_{m3}(\boldsymbol{q}, \boldsymbol{q}_1, \omega) + \phi^*(\boldsymbol{q}_1)P_{m4}(\boldsymbol{q}, \boldsymbol{q}_1, \omega)]\ \mathrm{d}\boldsymbol{q}_1 \qquad n = 1, 2 \tag{25}$$

$$X_{mn}(\boldsymbol{q}, \boldsymbol{q}', \omega) = \frac{2}{(2\pi)^2}\int [\phi(\boldsymbol{q}_1 - \boldsymbol{q}')\delta_{n3} + \phi^*(\boldsymbol{q}_1 - \boldsymbol{q}')\delta_{n4}]P_{mn}(\boldsymbol{q}, \boldsymbol{q}_1, \omega)\ \mathrm{d}\boldsymbol{q}_1 \qquad n = 3, 4 \tag{26}$$

where the structure factor $\phi(\boldsymbol{q})$ for the honeycomb structure is

$$\phi(\boldsymbol{q}) = \frac{1}{3}\{1 + \cos(q_2 a) + \cos(q_1 + q_2)a - \mathrm{i}[\sin(q_2 a) + \sin(q_1 + q_2)a]\}. \tag{27}$$

The corresponding equations for the random-walk theory have $\mathbf{X} = \mathbf{0}$ and $\mathbf{D} = D\mathbf{I}$ where $\mathbf{I}$ is the identity matrix. The probability functions for the random-walk theory of the honeycomb structure are then given immediately by $D\mathbf{Y}^{-1}$.

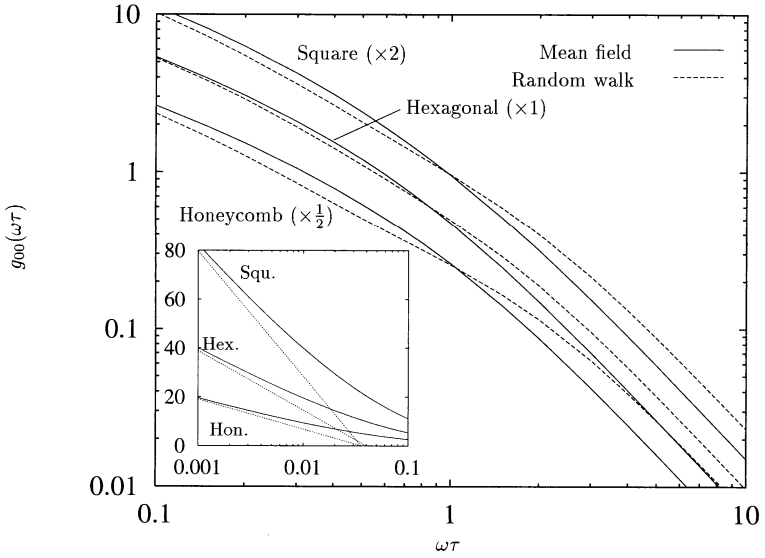

Figure 2. Spectral density functions $g_{00}(\omega\tau)$ for a simple random-walk model and the mean-field model on the square, hexagonal and honeycomb structures. The approach of the mean-field model to the $-\log(\omega\tau)$ limit for small $\omega\tau$ is shown in the inset. In all of these, the results for the square and honeycomb structures have been multiplied by 2 and 0.5 respectively for clarity.

To obtain the probability functions for the mean-field theory it is necessary to evaluate the matrix $\mathbf{X}$. This is achieved by defining $K_{mk}(\boldsymbol{q}, \omega)$ and $L_{mk}(\boldsymbol{q}, \omega)$ ($m = 1$ to 4, $k = 1$ to 3) to be

$$K_{mk}(\boldsymbol{q}, \omega) = \frac{1}{3(2\pi)^2}\int \mathrm{e}^{-\mathrm{i}\boldsymbol{q}_1\cdot\boldsymbol{p}_k}P_{m3}(\boldsymbol{q}, \boldsymbol{q}_1, \omega)\ \mathrm{d}\boldsymbol{q}_1 \tag{28}$$

$$L_{mk}(\boldsymbol{q}, \omega) = \frac{1}{3(2\pi)^2}\int \mathrm{e}^{\mathrm{i}\boldsymbol{q}_1\cdot\boldsymbol{p}_k}P_{m4}(\boldsymbol{q}, \boldsymbol{q}_1, \omega)\ \mathrm{d}\boldsymbol{q}_1 \tag{29}$$

and writing X_{mn} in terms of K_{mk} and L_{mk}. Substituting $(\mathbf{X}+\mathbf{D})\mathbf{Y}^{-1}$ for $\mathbf{P}$ into the integral definitions of K_{mk} and L_{mk} then provides a set of linear equations for them. The resulting equations show that $K_{mk}(\boldsymbol{q}) = L_{mk}(-\boldsymbol{q})$ and allow the calculation of the elements of $\mathbf{X}$. The final expressions for evaluating $P_{mn}(\boldsymbol{q}, \boldsymbol{q}', \omega)$ for the mean-field theory are given in the appendix.

4. Results

The probability functions in the previous section were used to calculate the spectral density functions $J_{00}(\omega)$ and $J_{22}(\omega)$, using equation (6), for the hexagonal lattice and honeycomb structure for both the random-walk and mean-field models. The high-frequency limit of these functions can be calculated independently of the above theory by considering the probabilities of zero or one jump of each of a pair of spins (Barton and Sholl 1980). This calculation was performed in all cases as a check on the results.

Table 1. Values of $a^6 S_{pp'}$ for the square, hexagonal and honeycomb structures where a is the distance between nearest-neighbour sites.

	Square	Hexagonal	Honeycomb
$a^6 S_{00}$	0.463 4307	0.634 2207	0.164 4276
$a^6 S_{22}$	0.695 1461	0.951 3310	0.246 6414
$a^6 S_{2-2}$	0.528 6311		

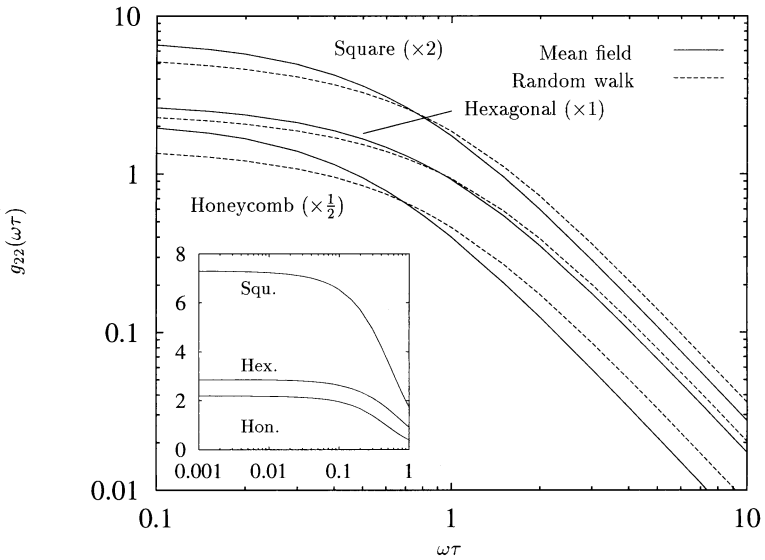

Figure 3. Spectral density functions $g_{22}(\omega\tau)$ for a simple random-walk model and the mean-field model on the square, hexagonal and honeycomb structures. The inset shows the mean-field results on a semi-logarithmic plot. The results for the square and honeycomb structures have been multiplied by 2 and 0.5 respectively for clarity.

The results are presented in terms of the dimensionless functions $g_{pp}(\omega\tau)$ defined by

$$J_{pp}(\omega) = c\tau S_{pp} g_{pp}(\omega\tau) \tag{30}$$

where $\tau = \tau_s/2$ and S_{pp} are constants which depend only on the geometry of the structure (SS). The values of S_{pp} are given in table 1.

Graphs of the calculated spectral density functions are shown in figures 2 and 3, which also include the results for the square lattice (SS) for comparison. As in the case of the square lattice, all functions show $1/(\omega\tau)^2$ behaviour in the large-$\omega\tau$ limit, $g_{22}(\omega\tau)$ approaches a constant as $\omega\tau \to 0$ and $g_{00}(\omega\tau)$ diverges as $\log(\omega\tau)$ in the small-$\omega\tau$ limit. The general forms of the functions are similar for all three structures and the magnitudes are also similar, so the results have been suitably scaled in the graphs to separate the curves. There are, however, differences in detail between the results for each structure and between the random-walk and mean-field results.

Table 2. Parameter values for the analytic approximation $g^a_{00}(\omega\tau)$ (equation (31)) for the random-walk (RW) and mean-field (MF) models of diffusion on the square, hexagonal and honeycomb structures. The maximum deviation, Δ, of g^a_{00} from the true spectral density function g_{00} in each case is also shown.

	Square		Hexagonal		Honeycomb	
	RW	MF	RW	MF	RW	MF
$\mathcal{A}$	0.412 6263	0.506 0716	0.432 0516	0.504 9257	0.405 7198	0.405 7182
$\mathcal{B}$	2.876 767	1.497 285	2.281 056	1.330 594	3.524 278	2.033 209
$\mathcal{C}$	28.0084	27.9817	25.8716	25.0542	27.6740	27.6740
v	27.0227	22.0330	24.3670	20.8502	26.1526	26.1527
a_1	$8.178\,25 \times 10^{-3}$	$9.192\,23 \times 10^{-2}$	$3.017\,88 \times 10^{-2}$	0.178 734	$2.971\,18 \times 10^{-3}$	0.320 254
a_2	$8.487\,36 \times 10^{-8}$	$1.780\,12 \times 10^{-5}$	$4.138\,57 \times 10^{-7}$	7.4955×10^{-5}	$3.792\,43 \times 10^{-8}$	$8.745\,31 \times 10^{-6}$
a_3	$1.441\,32 \times 10^{-14}$	$4.416\,63 \times 10^{-11}$	$7.186\,21 \times 10^{-14}$	$4.028\,84 \times 10^{-10}$	$1.968\,16 \times 10^{-14}$	$4.605\,14 \times 10^{-13}$
a_4	$1.630\,16 \times 10^{-22}$	$7.937\,99 \times 10^{-18}$	$2.642\,52 \times 10^{-21}$	$2.526\,97 \times 10^{-16}$	$2.710\,36 \times 10^{-22}$	$5.696\,88 \times 10^{-22}$
u_1	7.046 17	5.210 08	6.299 87	4.625 86	7.330 83	5.262 93
u_2	12.2001	9.386 60	11.5056	8.656 30	12.0553	10.6328
u_3	17.0250	13.4683	16.2262	12.7235	16.4586	15.9372
u_4	21.1932	17.0255	19.9545	16.1455	20.5911	20.5556
Δ	16.6%	2.7%	5.0%	2.9%	20.2%	5.5%

Analytic approximations for the functions have been developed so that they can be easily reproduced. These are

$$g^a_{00} = \mathcal{A}\log\left(1 + \frac{\mathcal{B}}{(\omega\tau)^2} + \frac{1}{(\mathcal{C}\omega\tau)^w} + \sum_{i=1}^{4}\frac{a_i}{(\omega\tau)^{u_i}}\right) \tag{31}$$

and

$$g^a_{2\pm2} = \frac{H}{a + b\omega\tau + c(\omega\tau)^u + d(\omega\tau)^v + (\omega\tau)^2} \tag{32}$$

where the values of $\mathcal{A}$, $\mathcal{B}$, $\mathcal{C}$, w, a_i, u_i, H, a, b, c, d, u and v are given in tables 2 and 3. The functional forms of the spectral density functions in the high- and low-frequency limits are modelled correctly by these functions. The maximum deviations of the approximations from the correct values (which occur at intermediate values of $\omega\tau$) are given in the tables.

It is of interest to determine how well a simple approximation of the type $\log[1 + 1/(\omega\tau)^2]$ can fit the functions. Firstly, this function is not suitable for J_{22} since this spectral

Table 3. Parameter values for the analytic approximation $g^a_{2\pm2}(\omega\tau)$ (equation (32)) for the random-walk (RW) and mean-field (MF) models of diffusion on the square, hexagonal and honeycomb structures. The maximum deviation, Δ, of $g^a_{2\pm2}$ from the true spectral density function $g_{2\pm2}$ in each case is also shown.

	g^a_{22}						g^a_{2-2}	
	Square		Hexagonal		Honeycomb		Square	
	RW	MF	RW	MF	RW	MF	RW	MF
H	1.815 078	1.385 794	2.066 703	1.753 021	1.695 424	1.090 465	1.902 251	1.337 744
a	0.637 591	0.379 143	0.818 592	0.615 645	0.561 737	0.248 707	0.794 866	0.387 051
b	−11.8938	−2.544 80	−28.0582	−28.0591	−7.209 38	−7.125 45	10.3291	−0.373 114
c	26.2052	−0.249 088	−13.8554	−13.8571	−8.448 15	−8.400 96	−9.283 21	−2.225 71
d	−13.9867	3.016 42	42.323	42.2117	15.9428	15.6497	−0.843 255	2.743 01
u	1.032 56	1.500 31	1.0769	1.1058	1.086 44	1.064 25	0.981 328	1.344 42
v	1.074 56	1.006 61	1.019 55	1.030 66	1.035 53	1.030 85	1.307 92	1.252 55
Δ	3.1%	3.2%	3.9%	5.0%	2.6%	0.81%	3.1%	4.2%

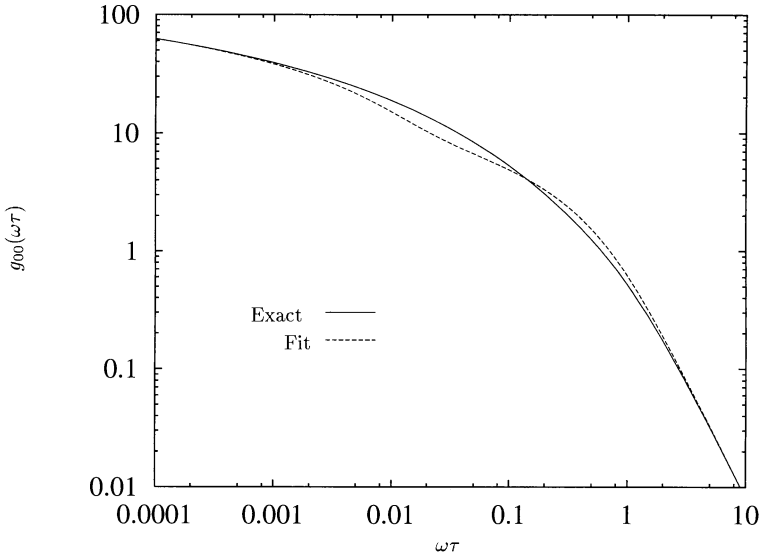

Figure 4. The spectral density function $g_{00}(\omega\tau)$ for the mean-field model on the honeycomb structure. The broken line shows the best fit of the function $g^R_{00}(\omega\tau)$ (equation (33)).

density function does not have a logarithmic divergence in the small-$\omega\tau$ limit. Secondly, a function $A\log[1 + B/(\omega\tau)^2]$ with only two parameters cannot fit $g_{00}(\omega\tau)$ in both the low-frequency limit, of the form $a_1 - b_1\log(\omega\tau)$, and the high-frequency limit, of the form $a_2/(\omega\tau)^2$. However, a modified function with four parameters, of the form

$$g^R_{00} = \sum_{i=1}^{2} A_i \log[1 + B_i/(\omega\tau)^2] \tag{33}$$

can fit both of these limits with an additional parameter to optimize the fit for intermediate values of $\omega\tau$. Values of the parameters A_i and B_i for this approximation are given in table 4

Table 4. Parameter values for the analytic approximation $g_{00}^{R}(\omega\tau)$ (equation (33)) for the random-walk (RW) and mean-field (MF) models of diffusion on the square, hexagonal and honeycomb structures. The maximum deviation, Δ, of g_{00}^{R} from the true spectral density function g_{00} in each case is also shown.

	Square		Hexagonal		Honeycomb	
	RW	MF	RW	MF	RW	MF
A_1	5.023 189	4.390 948	4.501 319	3.987 634	4.689 857	4.206 727
A_2	0.551 949	1.184 188	0.762 583	1.276 261	0.529 734	1.098 587
B_1	$5.635\,58 \times 10^{-4}$	$4.815\,41 \times 10^{-4}$	$4.752\,70 \times 10^{-4}$	$2.489\,99 \times 10^{-4}$	$5.427\,68 \times 10^{-4}$	$2.484\,85 \times 10^{-4}$
B_2	2.145 490	1.031 570	1.289 560	0.525 643	2.694 420	0.749 9320
Δ	44%	43%	37%	23%	36%	25%

and an example of the quality of the fit is shown in figure 4. The function is quite accurate for both small and large $\omega\tau$ but can have errors of $\sim$30% in the intermediate regions.

5. Conclusion

The spectral density functions calculated from the mean-field model provide an accurate means of analysing nuclear spin-relaxation data for like-spin magnetic dipolar interactions between spins undergoing translational diffusion on a two-dimensional hexagonal lattice or the honeycomb structure. The functions provide a rigorous solution for diffusion at low spin concentrations and are likely to be a reasonable approximation at other concentrations.

The method used for non-Bravais lattices could, in principle, be extended to more complex structures. This would be straightforward for the random-walk model, but the mean-field model is considerably more complicated and the increase in algebraic complexity and computing required for this model could be appreciable.

Appendix

The functions $L_{ij}(\omega)$ ($i, j = 1$ to 3) in equation (10) for the probability functions for the mean-field theory of the hexagonal lattice are

$$L_{11} = L_{22} = -K_5/(K_1K_2) \tag{A1}$$

$$L_{12} = L_{21} = -K_4/(K_1K_2) \tag{A2}$$

$$L_{13} = L_{23} = I_3/K_2 \tag{A3}$$

$$L_{31} = L_{32} = -K_3/(K_1K_2) \tag{A4}$$

$$L_{33} = K_6/K_2 \tag{A5}$$

where $K_i(\omega)$ ($i = 1$ to 6) are

$$K_1 = 1 - I_1 + I_2 \tag{A6}$$

$$K_2 = (1 - I_4)(1 - I_1 - I_2) - 2I_3^2 \tag{A7}$$

$$K_3 = I_3(I_1 - I_2 - 1) \tag{A8}$$

$$K_4 = I_4I_2 - I_2 - I_3^2 \tag{A9}$$

$$K_5 = I_3^2 - 1 + I_1 + I_4 - I_4I_1 \tag{A10}$$

$$K_6 = 1 - I_3 - I_2. \tag{A11}$$

The functions $I_i(\omega)$ ($i = 1$ to 4) are

$$I_i(\omega) = \frac{1}{3\tau(2\pi)^2}\int \mathrm{d}\boldsymbol{q}\ d_0(\boldsymbol{q},\omega)g_i(\boldsymbol{q}) \tag{A12}$$

where the functions $g_i(\boldsymbol{q})$ are

$$g_1(\boldsymbol{q}) = [1-\cos q_1 a]^2 \tag{A13}$$

$$g_2(\boldsymbol{q}) = 1 - 2\cos q_1 a + \cos q_1 a \cos q_2 a \tag{A14}$$

$$g_3(\boldsymbol{q}) = 1 - \cos q_1 a + \cos q_1 a \cos(q_1+q_2)a \tag{A15}$$

$$g_4(\boldsymbol{q}) = [1-\cos(q_1+q_2)a]^2. \tag{A16}$$

The probability functions for the mean-field theory of the honeycomb structure may be calculated from the following equations:

$$\mathbf{P} = (\mathbf{X}+\mathbf{D})\mathbf{Y}^{-1} \tag{A17}$$

$$X_{mn}(\boldsymbol{q},\omega) = -\sum_{k=1}^{3}[K_{mk}(\boldsymbol{q},\omega)+L_{mk}(\boldsymbol{q},\omega)] \qquad n = 1,2 \tag{A18}$$

$$X_{m3}(\boldsymbol{q},\boldsymbol{q}',\omega) = 2\sum_{k=1}^{3}\mathrm{e}^{\mathrm{i}\boldsymbol{q}'\cdot\boldsymbol{p}_k}K_{mk}(\boldsymbol{q},\omega) \tag{A19}$$

$$X_{m4}(\boldsymbol{q},\boldsymbol{q}',\omega) = 2\sum_{k=1}^{3}\mathrm{e}^{-\mathrm{i}\boldsymbol{q}'\cdot\boldsymbol{p}_k}L_{mk}(\boldsymbol{q},\omega) \tag{A20}$$

where the elements of the 4×3 matrices $\mathbf{K}$ and $\mathbf{L}$ are obtained from

$$\mathbf{M}(3\mathbf{I}+\mathbf{C}) = \mathbf{E} \tag{A21}$$

where the 4×6 block matrix $\mathbf{M} = (\mathbf{K},\mathbf{L})$. The matrix $\mathbf{I}$ is the 6×6 unit matrix, and the elements of $\mathbf{C}$ and $\mathbf{E}$ are

$$C_{jk} = 2U_k - 2V_{jk}^{(l)} \qquad l = \begin{cases} 1 & j \text{ and } k = 1,2,3 \text{ or } j \text{ and } k = 4,5,6 \\ 2 & \text{otherwise} \end{cases} \tag{A22}$$

$$E_{mk}(\boldsymbol{q},\omega) = 4\tau[F_{mk}(\boldsymbol{q},\omega) - U_k(\delta_{m,1}+\delta_{m,2})] \tag{A23}$$

where the functions F_{mk}, U_k and $V_{jk}^{(l)}$ are

$$F_{mk}(\boldsymbol{q},\omega) = \mathrm{e}^{-\mathrm{i}\boldsymbol{q}\cdot\boldsymbol{p}_k}NW\phi^* \qquad m = 1,2 \tag{A24}$$

$$F_{3k}(\boldsymbol{q},\omega) = \mathrm{e}^{-\mathrm{i}\boldsymbol{q}\cdot\boldsymbol{p}_k}N(W^2 - 2\phi\phi^*) \tag{A25}$$

$$F_{4k}(\boldsymbol{q},\omega) = \mathrm{e}^{-\mathrm{i}\boldsymbol{q}\cdot\boldsymbol{p}_k}2N(\phi^*)^2 \tag{A26}$$

$$U_k(\omega) = \frac{1}{(2\pi)^2}\int F_{1k}(\boldsymbol{q}_1,\omega)\ \mathrm{d}\boldsymbol{q}_1 \tag{A27}$$

$$V_{jk}^{(1)}(\omega) = \frac{1}{(2\pi)^2}\int \mathrm{e}^{\mathrm{i}\boldsymbol{q}_1\cdot\boldsymbol{p}_j}F_{3k}(\boldsymbol{q}_1,\omega)\ \mathrm{d}\boldsymbol{q}_1 \tag{A28}$$

$$V_{jk}^{(2)}(\omega) = \frac{1}{(2\pi)^2}\int \mathrm{e}^{-\mathrm{i}\boldsymbol{q}_1\cdot\boldsymbol{p}_j}F_{4k}(\boldsymbol{q}_1,\omega)\ \mathrm{d}\boldsymbol{q}_1 \tag{A29}$$

for j and $k = 1,2,3$ while for j and $k = 4,5,6$

$$F_{mk}(\boldsymbol{q},\omega) = F_{m,k-3}(\boldsymbol{q},\omega) \qquad m = 1,2,3,4 \tag{A30}$$

$$U_k(\omega) = U_{k-3}(\omega) \tag{A31}$$

$$V_k^{(l)}(\omega) = V_{k-3}^{(l)}(\omega) \qquad l = 1,2 \tag{A32}$$

and W, N and $\phi(\boldsymbol{q})$ are defined in section 3.

References

Barton W A and Sholl C A 1976 *J. Phys. C: Solid State Phys.* **9** 4315–28
——1980 *J. Phys. C: Solid State Phys.* **13** 2579–94
Ebinger H D, Jänsch H J, Polenz C, Polivka B, Preyss W, Saier V, Veith R and Fick D 1996 *Phys. Rev. Lett.* **76** 656–9
Fedders P A and Sankey O F 1978 *Phys. Rev.* B **18** 5938–47
Heitjans P, Faber W and Schirmer A 1991 *J. Non-Cryst. Solids* **131–133** 1053–62
Kimmerle F, Majer G, Kaess U and Maeland A J 1998 *J. Alloys Compounds* **264** 63–70
McDowell A F, Mendelsohn C F, Conradi M S, Bowman R C and Maeland A J 1995 *Phys. Rev.* B **51** 6336–42
Richards P M 1978 *Solid State Commun.* **25** 1019–21
Sholl C A 1981 *J. Phys. C: Solid State Phys.* **14** 447–64
——1986 *J. Phys. C: Solid State Phys.* **19** 2547–55
Stephenson P C L and Sholl C A 1993 *J. Phys.: Condens. Matter* **5** 2809–24